Draft version November 23, 2015
Preprint typeset using LaTeX style emulateapj v. 12/16/11

COLLISIONS KILL KAPPA: ELECTRON SPEED DISTRIBUTIONS IN PHOTOIONIZED NEBULAE

G. J. Ferland, W. J. Henney, C. R. O'Dell, M. Peimbert

Draft version November 23, 2015

ABSTRACT

Non-Maxwellian electron speed distributions have recently been suggested as a novel solution to long-standing discrepancies in the interpretation of emission line ratios from photoionized gas in H II regions and planetary nebulae. The power-law tailed κ distribution has been proposed as an alternative to temperature or abundance fluctuations as a means of reconciling the relative strengths of collisionally excited and recombination lines of the same ion. We show that the plasma collisionality in photoionized regions is so large (Knudsen number Kn = 10^{-10} to 10^{-6}) that deviations from a Maxwellian electron distribution have a negligible effect on diagnostic line ratios when integrated over an entire ionization-bounded nebula. This is true both for deviations induced by the photoionization/recombination process itself (including the case of a very hard ionizing continuum) and for any plausible scenario in which high-velocity electrons diffuse through the photoionized gas (for example, those originating in a hot shocked stellar wind bubble).

1. INTRODUCTION

Deviations from a Maxwellian electron velocity distribution in a plasma arise when significant non-local transport of electrons occurs, which is important if there are steep gradients in physical conditions (such as temperature). The dimensionless Knudsen number, Kn = λ/L, which describes the "collisionality" of the plasma, is the most important parameter in determining the importance of these deviations. This is the ratio between the electron elastic collisional mean free path, λ, and the relevant length scale, L, which is the distance over which physical conditions change appreciably (for instance, the scale length of the temperature gradient: $[d \ln T/ds]^{-1}$)

If Kn $\geq$ 1, then the plasma is "non-collisional" and the electron velocity distribution will be very different from a Maxwellian, and also non-isotropic in the presence of a significant magnetic field. An extreme example is the terrestrial magnetosphere, where Kn $\gg$ 1.

If Kn $<$ 1, then the plasma is "collisional" and as Kn $\rightarrow$ 0 the electron velocity distribution will tend towards a Maxwellian distribution at the local temperature. However, the fact that λ increases with electron velocity means that a significant high-energy non-Maxwellian tail can persist, even for rather small values of Kn. Quantities that are sensitive to this tail, such as thermal conductivity or the collisional excitation of optical/UV emission lines, can significantly deviate from the Maxwellian values for Kn as low as 0.001.

Theoretical explanations for the existence of kappa distributions as stationary equilibrium solutions to the Boltzmann equation have been found both for highly non-collisional (Kn $>$ 1) plasmas (Pierrard & Lazar 2010; Livadiotis & McComas 2013) and for mildly collisional (Kn $\sim$ 0.01) plasmas in the presence of stochastic turbulent electron acceleration (Bian et al. 2014).

In H II regions, Kn $\approx 1 \times 10^{-9}$ for the region as a whole, but certain sub-structures can have smaller values:

- Ionization fronts (where hydrogen rapidly changes from being prefominantly ionized to predominantly neutral) have Kn $\simeq 1 \times 10^{-6}$.
- Cooling zones behind moderate velocity (20–100 km s^{-1}) shocks also have Kn $\simeq 1 \times 10^{-6}$.

However, the emission from the both ionization fronts and post-shock cooling zones is typically only a tiny fraction of the total emission from the region (unless the ionization parameter is very low).

2. SUPRATHERMAL ELECTRONS IN SOLAR PHYSICS AND GEOPHYSICS

Summary of observations and modeling of the Transition Region, Coronal Loops, Solar Wind, and Terrestrial Magnetosphere.

Red dots show empirically estimated values of κ for the solar wind acceleration zone (Esser & Edgar 2000) (red dots, with the value for the innermost region at Kn = $2e-3$ being a lower limit)

3. THE COLLISIONALITY OF H II REGIONS AND STRUCTURES WITHIN THEM

As described in the introduction, the collisionality of a plasma is described by the Knudsen number Kn = λ/L. The relevant mean free path λ is the "deflection distance", which is the distance over which an electron's trajectory is deflected by 90° due to very many glancing Coulomb interactions with other charged particles (principally electrons and protons) in the plasma. For thermal electrons of temperature T_e and number density $n_e$this is given by

$$\lambda_0 = 2.625 \times 10^5 \frac{T_e^2}{n_e \ln \Lambda} \text{ cm} \quad (1)$$

where the slowly varying Coulomb logarithm ($\ln \Lambda = 9.452 + 1.5 \ln T_e - 0.5 \ln n_e$ for $T_e < 4.2 \times 10^5$ K) accounts for the cut-off in electrostatic interactions beyond the Debye radius. For a typical H II region temperature of $T_e = 10^4$ K this becomes $\lambda_0 \simeq 1.3 \times 10^{12} n_e^{-1}$ cm. This value is appropriate for electrons with velocities close to the mean thermal velocity $\langle u \rangle = \sqrt{2kT_e/m_e} \simeq 550$ km s^{-1} and with energies of order 1 eV. The deflection mean free path is substantially longer for higher energy electrons, scaling with velocity as u^4 or with energy as E^2.

We first estimate the Knudsen number for an idealised homogeneous dust-free ionization-bounded H II region by taking the scale length L as being the Strömgren radius $R_s = (3Q_H/4\pi\alpha_B n^2)^{1/3}$, where $n \simeq n_e$ is the ionized hydrogen density, Q_H is the rate of ionizing photons ($h\nu > 13.6$ eV) emitted by the source, and $\alpha_B \simeq 2.6 \times 10^{-13}$ cm^3 s^{-1} is the Case B

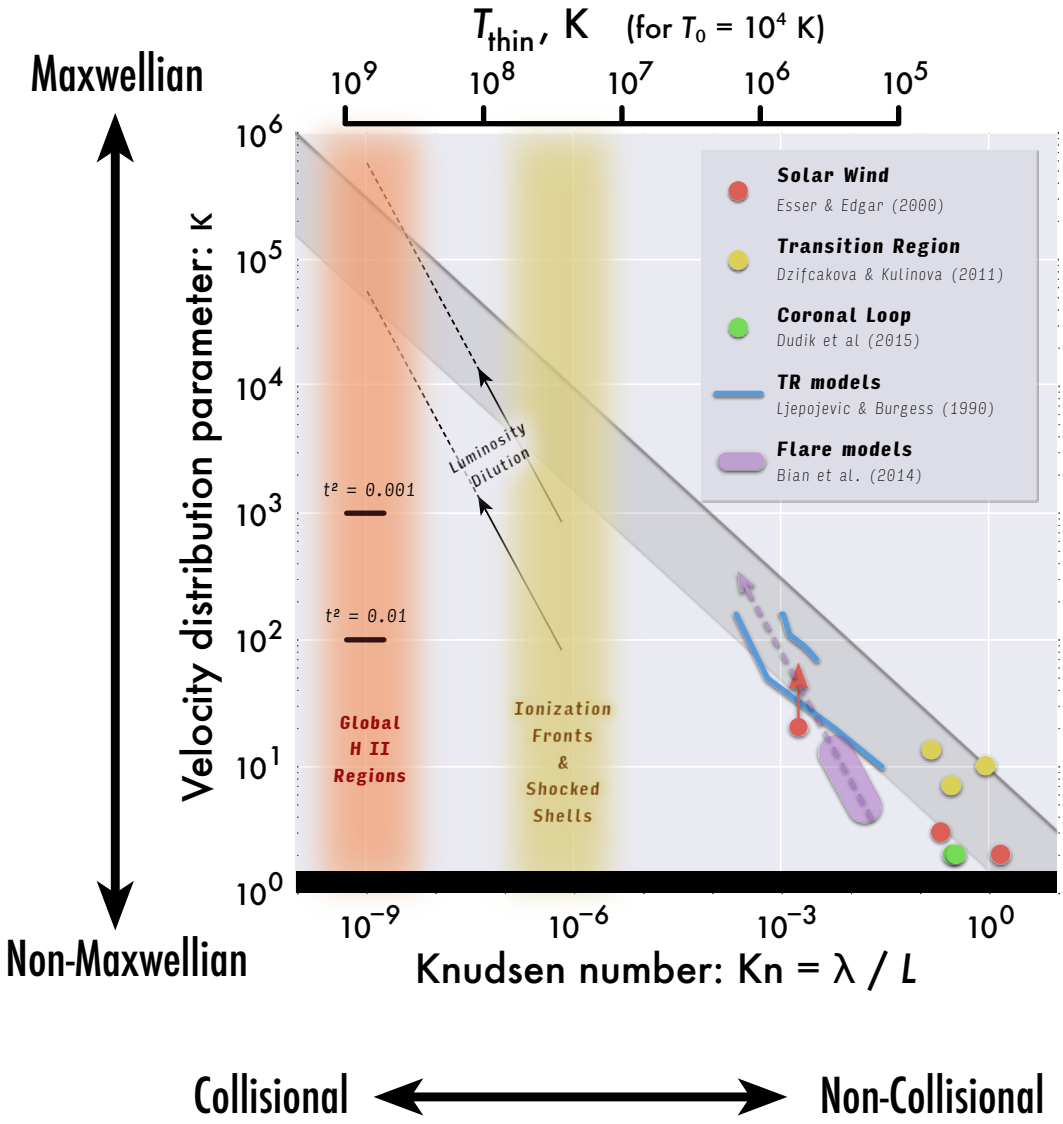

FIG. 1.— Location of H II regions and selected solar phenomena in the plane of Kappa (non-Maxwellian parameter) versus Knudsen number (plasma collisionality parameter). Colored dots show empirically estimated values of κ for the solar wind acceleration zone, the transition region between the chromosphere and corona, and for a coronal loop (see text for details). Colored lines show theoretical results from modelling non-local electron transport downwards through the transition region, and stochastic electron acceleration in solar flares (again, explained in more detail in the text). The diagonal darker gray band shows the relationship $\kappa \sim \mathrm{Kn}^{-1/2}$, which has no theoretical basis but which roughly captures the empirical trend seen in solar studies. H II regions and smaller-scale structures within them are represented by a fuzzy vertical bands to the left of the figure. The auxiliary horizontal scale at the top of the graph shows the temperature above which thermal electrons can freely stream along magnetic field lines over a length scale of order the size of the region (assuming background ionized gas at 10^4 K.)

TABLE 1
PHYSICAL CONDITIONS IN DIFFERENT CLASSES OF PHOTOIONIZED NEBULAE

Class	Example	Q_{49}	n	U
OB runaway nebula	ζ Oph/Sh 2-27	0.04	3	0.0003
Old planetary nebula	Helix Nebula	0.01	100	0.0006
Spitzer "Bubble"	RCW 120	0.3	1000	0.004
Compact H II region	Orion Nebula	1.0	10^4	0.02
Giant H II region	Carina, 30 Doradus	100	100	0.02
Super star cluster	Arches, M82 SSCs	1000	10^6	0.6

hydrogen recombination coefficient. We also introduce the global dimensionless ionization parameter $U = Q_H/4\pi R_s^2 nc$, where c is the speed of light, which is roughly an average ratio between the ionizing photon density and particle density in the nebula. We thus find $R_s = 3.46 \times 10^{23} U n^{-1}$ cm, from which it follows that the Strömgren Knudsen number is

$$\mathrm{Kn}_s = 3.76 \times 10^{-12} U^{-1},$$

which depends only on the ionization parameter and not on the density. It also follows from the above equations that the ionization parameter is $U \simeq 6 \times 10^{-4} (Q_{49} n)^{1/3}$, where Q_{49} is the ionizing luminosity normalized to 10^{49} s^{-1}, which is a typical value for a single O-type star. Values of Q_{49}, n, and U for different types of ionized nebulae are shown in Table 1.

vary from $U \simeq 0.0006$ for an evolved planetary nebula ($Q_{49} \simeq 0.01$, $n \simeq 100$ cm^{-3}) up to $U \simeq 0.02$ for a compact H II region ($Q_{49} \simeq 1$, $n \simeq 10^4$ cm^{-3}), implying $\mathrm{Kn}_s \approx 10^{-10}$–$10^{-8}$.

Super star clusters in M82 (McCrady & Graham 2007; Krumholz & Matzner 2009). OB runaway nebula (Gvaramadze et al. 2012). Spitzer bubble (Deharveng et al. 2009). Carina (Smith & Brooks 2008) 30 Dorados (Torres-Flores et al. 2013)

4. EQUILIBRIUM ELECTRON DISTRIBUTIONS IN PHOTOIONIZED PLASMAS

In a steady state homogeneous photoionized plasma, in the absence of external macroscopic forces, the electron velocity distribution function $\phi(u)$ will satisfy the equation:

$$\left(\frac{\partial\phi}{\partial t}\right)_{\rm elastic} + \left(\frac{\partial\phi}{\partial t}\right)_{\rm photo} + \left(\frac{\partial\phi}{\partial t}\right)_{\rm recomb} + \left(\frac{\partial\phi}{\partial t}\right)_{\rm inelastic} = 0, \quad (2)$$

where the four terms on the left hand side represent respectively elastic collisions, photoionization, recombination, and inelastic collisions. Note that the distribution function is normalized to $\int_0^\infty \phi(u) du = 1$. We now consider each individual term in detail.

Elastic collisions — $(\partial\phi/\partial t)_{\rm elastic}$ is the traditional collisional redistribution integral in the Boltzmann equation (e.g., Pitaevskii & Lifshitz 1981), also known as the Fokker–Planck operator, which tends to drive the velocity distribution towards thermal equilibrium. A rigorous treatment of this term is difficult and we instead adopt the BGK approximation, first introduced by Bhatnagar et al. (1954), in which the collision integral is replaced by a simple relaxation toward a Maxwellian distribution $\phi^*(u)$:

$$\left(\frac{\partial\phi}{\partial t}\right)_{\rm elastic} = -\frac{1}{\tau}(\phi - \phi^*), \quad (3)$$

where $\tau = \lambda/u$ is the elastic collisional timescale. This is a source term ($(\partial\phi/\partial t)_{\rm elastic} > 0$) at velocities where the distribution is sub-Maxwellian ($\phi < \phi^*$) and is a sink term ($(\partial\phi/\partial t)_{\rm elastic} < 0$) at velocities where the distribution is supra-Maxwellian ($\phi > \phi^*$). Thus, acting alone, $(\partial\phi/\partial t)_{\rm elastic}$ would drive the electrons to a Maxwellian distribution, $\phi \to \phi^*$, on a timescale τ.

Since the BGK approximation is only phenomonelogical, different possible choices exist for the exact form of the relaxation timescale τ. Livi & Marsch (1986) compared the BGK approximation with evaluation of the full Fokker-Planck operator when calculating the time-dependent relaxation of initially anisotropic bi-Maxwellian and double-beam configurations. They found that the closest correspondence was obtained by using the velocity-space friction timescale τ_F (Spitzer 1956, chapter ???), and so we adopt that timescale in this work. If ξ is the electron velocity expressed in units of the mean thermal speed ($\xi = u/\langle u\rangle$) then

$$\tau_F = \frac{\tau_0\, \xi^2}{\mathrm{erf}\, \xi - \xi\, \mathrm{erf}'\xi}, \quad (4)$$

where $\tau_0 = \lambda_0/\langle u\rangle$, with λ_0 given by equation (1), and erf, erf$'$ are respectively the error function and its derivative. This timescale diverges both for very small and very large velocities:

$$\lim_{u\to 0} \tau_F \propto u^{-1} \quad \text{and} \quad \lim_{u\to\infty} \tau_F \propto u^2, \quad (5)$$

meaning that elastic collisions take longer to Maxwellianize the low-energy and high-energy tails of the distribution.

Photoionizations — $(\partial\phi/\partial t)_{\rm photo}$ represents the rate of production of photo-electrons with velocity u due to the photoionization of neutral hydrogen or atoms/ions of other elements. Consider the photoionization of H from the ground level (see Osterbrock & Ferland 2006, § 2.3) by photons of energy $h\nu$. The resultant photo-electron will have energy $\frac{1}{2} m_e u^2 = h\nu - h\nu_0$, where $h\nu_0 = 13.6$ eV is the H ionization potential.

If J_ν is the mean intensity of the radiation field and $n(\mathrm{H}^0)$ is the number density of neutral H, then the contribution due tois

$$\left(\frac{\partial\phi}{\partial t}\right)_{\rm photo} = n(\mathrm{H}^0) \frac{4\pi J_\nu}{h\nu} a_\nu \frac{d\nu}{du}, \quad (6)$$

where =.

5. DIFFUSION OF HIGH ENERGY ELECTRONS THROUGH PHOTOIONIZED GAS

5.1. *Cooling zone behind low-velocity shocks*

Spitzer–Härm approximation is valid for $\xi < \xi_c = \mathrm{Kn}_T^{-1/4}$ (Shoub 1983), where the temperature-gradient Knudsen number is $\mathrm{Kn}_T = \lambda_0 d \ln T/dz$. So, with Kn = 0.0065 which I get from the shock models, we find $\xi_c = 3.5$. Thus, for $\xi < 3.5$ we have

$$\phi(\xi, \mu, z) = \phi^*(\xi, z)\Big[1 + \mu\, \mathrm{Kn}\, D(\xi) + O(\mathrm{Kn}^2)\Big] \quad (7)$$

where $D(\xi)$ is given in Table II of Spitzer & Härm (1953). This implies that the deviation of the angle-averaged distribution function from Maxwellian is of order $(\mathrm{Kn})^2$ for $\xi < \xi_c$.

We should check this against results of BGK calculations.

5.2. *Leakage of hot electrons from stellar wind bubbles*

Recent models of stellar wind bubbles inside H II regions (Mackey et al. 2015)

Survey of H II regions in LMC and SMC (Lopez et al. 2014) give X-ray emitting hot gas with $T = 2$–8×10^6 K and density 0.01–0.3 cm^{-3}. *Also look at* ... Carina (Townsley et al. 2011)

REFERENCES

Bhatnagar, P. L., Gross, E. P., & Krook, M. 1954, Physical Review, 94, 511
Bian, N. H., Emslie, A. G., Stackhouse, D. J., & Kontar, E. P. 2014, ApJ, 796, 142
Deharveng, L., Zavagno, A., Schuller, F., Caplan, J., Pomarès, M., & De Breuck, C. 2009, A&A, 496, 177
Esser, R., & Edgar, R. J. 2000, ApJ, 532, L71
Gvaramadze, V. V., Langer, N., & Mackey, J. 2012, MNRAS, 427, L50
Krumholz, M. R., & Matzner, C. D. 2009, ApJ, 703, 1352
Livadiotis, G., & McComas, D. J. 2013, Space Sci. Rev., 175, 183
Livi, S., & Marsch, E. 1986, Phys. Rev. A, 34, 533
Lopez, L. A., Krumholz, M. R., Bolatto, A. D., Prochaska, J. X., Ramirez-Ruiz, E., & Castro, D. 2014, ApJ, 795, 121
Mackey, J., Gvaramadze, V. V., Mohamed, S., & Langer, N. 2015, A&A, 573, A10
McCrady, N., & Graham, J. R. 2007, ApJ, 663, 844
Osterbrock, D. E., & Ferland, G. J. 2006, Astrophysics of gaseous nebulae and active galactic nuclei, 2nd edn. (Sausalito, CA: University Science Books)
Pierrard, V., & Lazar, M. 2010, Sol. Phys., 267, 153
Pitaevskii, L., & Lifshitz, E. 1981, Course of Theoretical Physics, Vol. 10, Physical Kinetics, ed. L. Landau & E. Lifshitz (Pergamon Press)
Shoub, E. C. 1983, ApJ, 266, 339
Smith, N., & Brooks, K. J. 2008, The Carina Nebula: A Laboratory for Feedback and Triggered Star Formation, ed. B. Reipurth, 138–+
Spitzer, L. 1956, Physics of Fully Ionized Gases
Spitzer, L., & Härm, R. 1953, Physical Review, 89, 977
Torres-Flores, S., Barbá, R., Maíz Apellániz, J., Rubio, M., Bosch, G., Hénault-Brunet, V., & Evans, C. J. 2013, ArXiv e-prints
Townsley, L. K., Broos, P. S., Chu, Y.-H., Gruendl, R. A., Oey, M. S., & Pittard, J. M. 2011, ApJS, 194, 16